บทความวิจัย

การเตรียมกระเบื้องเซรามิกอย่างยั่งยืนเผาที่อุณหภูมิต่ำโดยใช้เถ้าลอยจากเตาเผาขยะชุมชน เศษแก้วสีเขียว และดินขาวลำปาง

ภูริณัฐ ใหม่งาม และ ณัฐกฤตา ปิยะรัตน์*
ภาควิชาวิศวกรรมการผลิตและหุ่นยนต์ คณะวิศวกรรมศาสตร์ มหาวิทยาลัยเทคโนโลยีพระจอมเกล้าพระนครเหนือ

* ผู้นิพนธ์ประสานงาน โทรศัพท์ 0 2555 2000 ต่อ 8218 อีเมล: natthakitta.p@eng.kmutnb.ac.th DOI: 10.14416/j.kmutnb.2026.07.001
รับเมื่อ 19 ธันวาคม 2568 แก้ไขเมื่อ 18 มีนาคม 2569 ตอบรับเมื่อ 1 เมษายน 2569 เผยแพร่ออนไลน์ 24 กรกฎาคม 2569

บทคัดย่อ

งานวิจัยนี้ศึกษาความเป็นไปได้ในการผลิตกระเบื้องเซรามิกอย่างยั่งยืน โดยใช้เถ้าลอยจากเตาเผาขยะชุมชน เศษแก้วสีเขียว และดินขาวลำปาง ออกแบบส่วนผสมด้วยส่วนผสมสามส่วน จำนวน 10 สูตร แบ่งออกเป็น 4 กลุ่ม ตามปริมาณเถ้าลอยร้อยละ 0 10 20 และ 30 ขึ้นรูปชิ้นงานด้วยเครื่องอัดแบบทางเดียว แรงดัน 10 เมกะปาสกาล เผาที่อุณหภูมิ 850 องศาเซลเซียส และ 950 องศาเซลเซียส ทดสอบคุณสมบัติทางกายภาพ ได้แก่ ความแข็งแรงดัด การดูดซึมน้ำ การหดตัวเชิงเส้น การสูญเสียน้ำหนักหลังเผา และความหนาแน่นรวม จากนั้นเปรียบเทียบคุณสมบัติตามมาตรฐาน EN 14411 ผลการทดลองพบว่าสูตรที่ไม่มีเถ้าลอยและมีเศษแก้วสีเขียวร้อยละ 60–70 เผาที่ 850 องศาเซลเซียส และร้อยละ 50–70 เผาที่ 950 องศาเซลเซียส สามารถผ่านเกณฑ์มาตรฐาน EN 14411 ทั้งด้านความแข็งแรงดัดและการดูดซึมน้ำ อีกทั้งสูตรที่มีเถ้าลอยร้อยละ 10 เผาที่ 850 องศาเซลเซียส และร้อยละ 20 เผาที่ 950 องศาเซลเซียส สามารถผ่านเกณฑ์มาตรฐาน EN 14411 ได้เช่นกัน การวิเคราะห์ด้วยกล้องจุลทรรศน์แบบออปติคัลแสดงการเกิดเฟสแก้ว และความหนาแน่นเพิ่มขึ้นตามอุณหภูมิการเผาที่สูงขึ้น นอกจากนี้ออกไซด์ฟลักซ์ที่มีแคลเซียมออกไซด์สูงจากเศษแก้ว และเถ้าลอยจากเตาเผาขยะชุมชนอาจช่วยส่งเสริมตรึงโลหะหนักภายในโครงสร้างเซรามิก ซึ่งสนับสนุนการผลิตกระเบื้องเซรามิกอย่างยั่งยืน การเผาที่ใช้พลังงานอย่างมีประสิทธิภาพ และการใช้ประโยชน์จากของเสียอย่างมีประสิทธิผล

คำสำคัญ: กระเบื้องเซรามิกอย่างยั่งยืน ดินขาว เถ้าลอยจากเตาเผาขยะชุมชน เผาที่อุณหภูมิต่ำ เศษแก้ว

การอ้างอิงบทความ: ภูริณัฐ ใหม่งาม และ ณัฐกฤตา ปิยะรัตน์, "การเตรียมกระเบื้องเซรามิกอย่างยั่งยืนเผาที่อุณหภูมิต่ำโดยใช้เถ้าลอยจากเตาเผาขยะชุมชน เศษแก้วสีเขียว และดินขาวลำปาง," *วารสารวิชาการพระจอมเกล้าพระนครเหนือ*, ปีที่ 36, ฉบับที่ 4, หน้า 1–20, ต.ค.–ธ.ค. 2569. เลขที่บทความ 264-028252, doi: 10.14416/j.kmutnb.2026.07.001.

Research Article

Preparation of Low-Temperature-Fired Sustainable Ceramic Tiles Using Municipal Waste Incineration Fly Ash, Green Glass Waste, and Lampang Kaolin

Purinut Maingam and Natthakitta Piyarat*

Department of Production and Robotics Engineering, Faculty of Engineering, King Mongkut's University of Technology North Bangkok, Bangkok, Thailand

* Corresponding Author, Tel. 0 2555 2000, Ext. 8218, E-mail: natthakitta.p@eng.kmutnb.ac.th
DOI: 10.14416/j.kmutnb.2026.07.001

Received 19 December 2025; Revised 18 March 2026; Accepted 1 April 2026; Published online: 24 July 2026

Abstract

This study examines the feasibility of producing sustainable ceramic tiles using Municipal Solid Waste Incineration Fly Ash (MSWI FA), Green Glass Waste (GGW), and Lampang Kaolin (LK). Ten experimental mixtures were formulated using a ternary mixture design and categorized into four series with MSWI FA contents of 0, 10, 20, and 30%, respectively. The specimens were uniaxially pressed at 10 MPa and subsequently fired at 850°C and 950°C. The physical properties, including flexural strength, water absorption, linear shrinkage, weight loss after firing, and bulk density, were evaluated. In addition, flexural strength and water absorption were compared with the requirements of the EN 14411 standard for ceramic tiles. The results indicate that mixtures without MSWI FA, containing 60–70% GGW when fired at 850°C and 50–70% GGW when fired at 950°C, satisfied the EN 14411 requirements for both flexural strength and water absorption. Moreover, mixtures incorporating 10% MSWI FA fired at 850°C and 20% MSWI FA fired at 950°C also met the EN 14411 criteria. Optical microscopy supported these findings by revealing enhanced glassy phase formation and increased densification at higher firing temperatures. Furthermore, the combined CaO-rich fluxing oxides derived from GGW and MSWI FA may facilitate the stabilization of hazardous heavy metals within the ceramic matrix, thereby supporting sustainable ceramic tile production, energy-efficient firing, and effective waste valorization.

Keywords: Sustainable Ceramic Tiles, Kaolin, MSWI Fly Ash, Low-Temperature-Fired, Glass Waste

Please cite this article as: P. Maingam and N. Piyarat, "Preparation of low-temperature-fired sustainable ceramic tiles using municipal waste incineration fly ash, green glass waste, and Lampang Kaolin," *The Journal of KMUTNB*, vol. 36, no. 4 pp. 1–20, Oct.–Dec. 2026 (in Thai), Art. no. 264-028252, doi: 10.14416/j.kmutnb.2026.07.001.

1. Introduction

In 2024, global ceramic tile production reached 14.95 billion m², with Asia producing 10.9 billion m², accounting for 72.8% of total output. However, defect rates exceeding 7%, mainly caused by suboptimal raw material selection and poor kiln temperature control, generate substantial ceramic waste during manufacturing [1]. Meanwhile, the global generation of Municipal Solid Waste (MSW) has increased rapidly as a result of economic growth and urbanization. Approximately 1.3 billion tons of MSW were produced in 2012, increasing to about 2.2 billion tons annually in recent years, and this volume is projected to exceed 3.8 billion tons per year by 2050 [2]. During waste incineration, Municipal Solid Waste Incineration (MSWI) fly ash is unavoidably generated, representing about 1–3% of the initial MSW mass [3]. MSWI fly ash is classified as hazardous waste due to its content of heavy metals and toxic organic compounds. Therefore, its disposal poses a critical environmental challenge and has prompted extensive research into various treatment and utilization methods for reducing ash volume, such as landfilling, fluxing, sintering, melting, and cement solidification [4]. Despite these efforts, recycling rates remain low because of the high impurity content of MSWI fly ash. However, MSWI fly ash contains valuable oxides, including SiO_2, Al_2O_3, CaO, and Fe_2O_3, making it a potential low-cost resource for glass and ceramic products. Most studies report that the utilization efficiency of MSWI fly ash is limited to 10–20% [5]. Additionally, while the addition of MSWI fly ash to cementitious materials has shown potential, previous studies indicate that the feasible addition of untreated MSWI fly ash is restricted to around 10% [6]. Melting treatment technology has been proposed to immobilize hazardous components by transforming MSWI fly ash into a vitrified slag at 1100–1500°C, during which heavy metals are either volatilized or stabilized [7]. Nevertheless, the melting point of MSWI fly ash exceeds 2400°C because of its high CaO content [8], leading to excessive energy consumption and the need for auxiliary materials to reduce melting temperature.

Waste glass is another significant solid waste stream, primarily derived from glass containers and single-use drinking items with short product lifespans. Although waste glass can be recycled to create new glass products, a substantial amount is still disposed of in landfills. It is estimated that approximately 30% of global waste glass is landfilled due to color variations, impurities, and the high cost of sorting and reprocessing, which collectively result in low recycling efficiency [9]. When crushed into fine particles, waste glass of various colors (green, brown, etc.) can be used as a substitute for sand in applications such as sandblasting, water filtration, aggregates, bricks, and tiles [10]. Moreover, waste glass has the potential to act as a fluxing agent owing to its high contents of Na_2O, K_2O, and CaO, which can effectively reduce the melting point of ceramic raw materials, including stoneware, bricks, and tiles [11]. When incorporated with clay-based materials, waste glass can lower the sintering temperature and consequently reduce energy consumption in ceramic production [9]. Several studies have reported that incorporating 50–70% waste glass with rice husk ash and kaolin, followed by firing at 900°C [12] and 1050°C [13], can reduce the firing temperature by 50–100°C while enabling the physical properties of ceramic tiles to meet the requirements of the ISO 13006 standard.

Despite the promising use of MSWI fly ash and waste glass in ceramic materials, previous studies have mainly investigated them individually, often with relatively low MSWI fly ash contents and high firing temperatures. Moreover, the synergistic potential of integrating multiple waste streams as fluxing agents in ceramic tile production remains insufficiently explored.

In this study, sustainable ceramic tiles were developed using a ternary mixture design comprising Municipal Solid Waste Incineration Fly Ash (MSWI FA), Green Glass Waste (GGW), and Lampang Kaolin (LK). The synergistic fluxing oxides in MSWI FA and GGW were utilized to promote sintering at relatively low firing temperatures of 850°C and 950°C. The physical properties of the fired specimens were evaluated according to the EN 14411 standard for ceramic tile classification, and their microstructures were examined using optical microscopy. This work provides a systematic evaluation of low-temperature ceramic tile production through dual waste incorporation, offering a promising pathway toward circular waste utilization and energy-efficient ceramic manufacturing.

2. Materials and Methods

2.1 Chemical Composition Analysis

All raw materials used in this study were sourced in Thailand. The chemical compositions of the raw materials were analyzed by X-Ray Fluorescence (XRF) using the Wavelength Dispersive X-Ray Fluorescence (WDXRF) method at the Nuclear Technology Service Center, Thailand Institute of Nuclear Technology (Public Organization), as presented in Table 1.

MSWI FA was collected from a municipal solid waste incineration plant, and its major

Table 1 Chemical compositions of raw materials.

Oxides	MSWI FA (%)	GGW (%)	LK (%)
SiO_2	45.81	69.91	72.13
Na_2O	0.62	14.64	0.26
CaO	14.12	10.81	0.09
Al_2O_3	10.61	1.91	17.43
MgO	1.68	1.24	0.09
K_2O	1.52	0.36	3.06
Fe_2O_3	9.96	0.43	0.67
Cr_2O_3	-	0.30	-
BaO	-	0.09	-
TiO_2	1.50	0.08	0.03
SO_3	2.84	0.07	-
SrO	-	0.04	-
ZrO_2	-	0.03	-
P_2O_5	1.08	-	-

chemical constituents are SiO_2, CaO, Al_2O_3, and Fe_2O_3. Hence, MSWI FA is considered suitable as a blending agent for ceramic tile production, particularly in compositions based on the SiO_2-CaO-Al_2O_3-Fe_2O_3 system, due to its compositional similarity to conventional ceramic raw materials [14]. GGW was sourced from a local glass recycling facility. It serves as a primary source of SiO_2 for ceramics and meets the compositional requirements of basic ceramic materials. In addition, GGW contains notable alkali oxides (Na_2O, K_2O, and CaO), which act as strong fluxing agents, promoting melt formation and reducing the melting point of raw materials. LK was obtained from Lampang

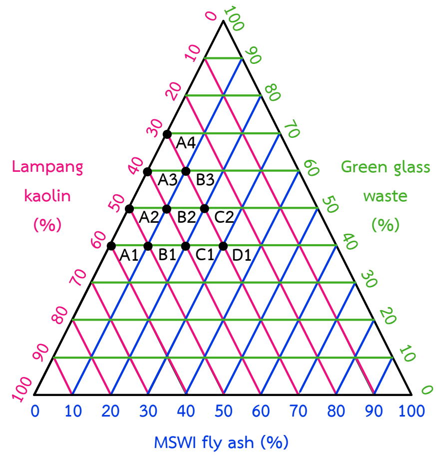

Figure 1 Ternary diagram showing of mixture compositions using MSWI fly ash, green glass waste, and Lampang kaolin.

province. It is rich in SiO_2 and Al_2O_3, which improve plasticity and facilitate the forming process of ceramic bodies [15].

2.2 Experimental Mixture Design

A ternary mixture design was employed to develop the experimental mixtures using MSWI FA, GGW, and LK as the primary raw materials. A total of ten mixtures were prepared and systematically positioned within the ternary diagram for the A-D series, as shown in Figure 1.

The mixtures were categorized into four series (A, B, C, and D) according to MSWI FA contents of 0, 10, 20, and 30%, respectively, while GGW and LK constituted the remaining compositions, as shown in Table 2. These proportions were selected based on literature benchmarks indicating that the utilization efficiency of MSWI FA is typically limited to about 10–25% [5], [16]. In this study, the MSWI FA content was extended to 30% to assess the feasibility of increasing its recycling rate in environmentally friendly ceramic products, supported by preliminary flexural strength results. The compositions were designed to investigate the effect of increasing MSWI FA content on ceramic properties by systematically varying the ratio of GGW, serving as the primary fluxing agent, and LK, functioning as the main structural component.

Table 2 Mixture compositions.

Mix	MSWI FA (%)	GGW (%)	LK (%)
A1	0	40	60
A2	0	50	50
A3	0	60	40
A4	0	70	30
B1	10	40	50
B2	10	50	40
B3	10	60	30
C1	20	40	40
C2	20	50	30
D1	30	40	30

2.3 Methods

All raw materials were initially dried in an electric oven at 200°C to remove moisture and then ground under dry conditions at 100 rpm using a ball mill. The resulting powders were sieved through a 50 mesh (297 μm) sieve using a sieve shaker. The dry powders were homogeneously mixed with water for all ten mixtures. Approximately 10% water was added onto the mixtures to obtain sufficient consistency for the pressing process. Rectangular specimens were fabricated by uniaxial hydraulic pressing at 10 MPa, producing specimens with dimensions of 50 × 100 × 7 mm. For each mixture, fifteen specimens were prepared for drying and sintering. The specimens were dried at 200°C for 2 h to remove residual moisture, followed by sintering at 850°C and 950°C with a heating rate of 100°C/h. The maximum temperature was held for 1 h, after which the specimens were cooled to room temperature.

After sintering, the specimens were characterized to evaluate their properties, including fluxing agent, flexural strength (ISO 10545-4), water absorption (ISO 10545-3), linear shrinkage (ISO 10545-3), weight loss, and bulk density (ISO 10545-3). The flexural strength and water absorption results were compared with the requirements specified in the EN 14411 standard for ceramic tiles. XRF analysis was also performed to analyze the chemical compositions of the dried powders using a WDXRF spectrometer S8 TIGER (Bruker, Germany) under vacuum conditions [12]. Surface microstructural features were examined using an Olympus DSX1000 optical microscope. Images were captured in polarization mode with an Olympus DSX10-XLOB Plan FL10×/0.30 WD 30 lens at magnifications of 150× and 300×, enabling a comparative evaluation of matrix consolidation, sintering behavior, and porosity.

2.4 Property Testing and Standardized Requirements

The fluxing agent content was calculated based on the oxides of Na_2O, K_2O, and CaO obtained from the XRF analysis of each raw material, together with their respective proportions in the mixture [12]. Specifically, the oxide percentage of each material was multiplied by its weight ratio in the mixture to calculate the fluxing oxides. For example, in mix A1, MSWI FA was not included, while GGW at 40% and LK at 60% accounted for 10.324% and 2.046% of the total fluxing oxide content, respectively. The total calculated fluxing agent content was determined by summing these values, resulting in a value of 12.37%. A summary of the calculated fluxing agent content for mix A1 is provided in Table 3.

Flexural strength (R), or modulus of rupture, was determined using a three-point flexural test. This parameter represents the breaking load applied at the center of the sample with the load recorded at the point of

Table 3 Calculation of fluxing agent for mix A1.

Calculation of fluxing agent for mix A1					
Materials	Ratio (%)	Oxide contents (%)			Fluxing oxide (%)
		Na_2O	K_2O	CaO	
MSWI FA	0	0.62	1.52	14.12	0
GGW	40	14.64	0.36	10.81	10.324
LK	60	0.26	3.06	0.09	2.046
Total calculated fluxing agent (%)					12.37

failure. The test was conducted using a support span (l_2) of 80 mm in accordance with the ISO 10545-4 standard. The R was evaluated using Equation (1).

$$R = \frac{3Fl_2}{2bh^2} \tag{1}$$

Where; R = flexural strength (MPa)

F = the breaking load (N)

l_2 = the span between the support rods (mm)

b = the width of sample (mm)

h = the minimum thickness of sample (mm)

Water absorption (E_v) is defined as the ratio of the mass of absorbed water to the mass of the dry sample. It was evaluated in accordance with the ISO 10545-3 standard. First, the mass of the dry sample (W_d) was recorded. The samples were then boiled in distilled water at 105°C for 2 h and subsequently soaked for 24 h at room temperature. After impregnation, the mass of the wet sample (W_w) was measured. The E_v was calculated using Equation (2).

$$E_v = \frac{W_w - W_d}{W_d} \times 100 \qquad (2)$$

Where; E_v = water absorption (%)

W_w = the mass of wet sample (g)

W_d = the mass of dry sample (g)

Linear shrinkage (LS) was quantified as the percentage reduction in sample length measured with a caliper, following the ISO 10545-3 standard. The LS test was performed by comparing the length of the sample before and after firing. The LS was evaluated using Equation (3).

$$LS = \frac{L_0 - L}{L_0} \times 100 \qquad (3)$$

Where; LS = linear shrinkage (%)

L_0 = the length of sample before firing (mm)

L = the length of sample after firing (mm)

Weight loss (WL) was expressed as the percentage reduction in mass by comparing the initial mass of the sample before firing with its final mass after firing. The WL was calculated using Equation (4).

$$WL = \frac{W_1 - W_2}{W_1} \times 100 \qquad (4)$$

Where; WL = weight loss (%)

W_1 = the weight of sample before firing (g)

W_2 = the weight of sample after firing (g)

Bulk density (B) was assessed as the ratio of the dry mass to the exterior volume of the sample, which includes solid material and pore volume. Measurements followed the ISO 10545-3 standard using Archimedes' principle and a densimeter (Alfa Mirage, EW-300SG). The B value was subsequently calculated using Equation (5).

$$B = \frac{m}{v} \qquad (5)$$

Where; B = bulk density (g/cm^3)

m = the dry mass of sample (g)

v = the exterior volume (cm^3)

The EN 14411 standard for ceramic tiles, which is aligned with the ISO 13006 standard specification, classifies products manufactured by the dry pressing technique under method B. The measured flexural strength (R) and water absorption (E_v) values of the specimens were then compared with the EN 14411 requirements [17]. The classification criteria for flexural strength and water absorption are presented in Table 4.

Table 4 Classification requirements of flexural strength and water absorption with the EN 14411 standard for ceramic tiles.

Group	Flexural strength, R (MPa)	Water absorption, E_v (%)
BI_a	$R \geq 35$	$E_v \leq 0.5$
BI_b	$R \geq 30$	$0.5 < E_v \leq 3$
BII_a	$R \geq 22$	$3 < E_v \leq 6$
BII_b	$R \geq 18$	$6 < E_v \leq 10$
BIII	$R \geq 15$	$10 > E_v$

3. Results and Discussions

The physical properties of all mixtures were evaluated across four series (A–D). For each test, the mean values and Standard Deviation (SD) were calculated from 15 specimens (n = 15), as shown in Figures (3)–(7). The fluxing agent content was calculated and is therefore reported without a standard deviation. The Relative Standard Deviation (RSD) for all measured properties was below 10%, indicating acceptable experimental repeatability [18].

3.1 Fluxing Agent

The fluxing agent content was determined from the combined concentrations of alkali and alkaline earth oxides (Na_2O, K_2O, and CaO) in the raw materials and was calculated according to their respective mixing ratios. As shown in Figure 2, the total fluxing oxide content ranged from 12.37% to 19.09%. In the A series, the fluxing agent content increased steadily from A1 to A4 as the proportion of GGW rose. For instance, mix A1 containing 40% GGW had the lowest fluxing agent value at 12.37%, whereas increasing the GGW content to 70% in mix A4 yielded the highest value of 19.09%. When comparing mixtures with an identical GGW content of 40% (A1, B1, C1, and D1), the fluxing agent values were 12.37%, 13.66%, 14.94%, and 16.23%, respectively, showing a progressive increase with increasing MSWI FA content due to the systematic replacement of LK with MSWI FA. The higher fluxing oxide content from GGW and MSWI FA promotes glassy phase formation, particle bonding, compaction, and strength [19]. Previous studies have reported that CaO-rich compositions enhance crystallization and stabilize hazardous elements (e.g., Cr and Pb) within the ceramic matrix, thereby reducing heavy-metal leaching and contributing to the immobilization of toxic metals after sintering [20]. In this study, the relatively high combined CaO contribution from GGW and MSWI FA may further facilitate the immobilization of hazardous metals within the ceramic structure. In contrast, LK is characterized by a minimal presence of compounds contributing to thermal expansion, a high melting point, and a high content of refractory oxides such as SiO_2 and Al_2O_3. As a result, increasing the proportion of LK lowers the fluxing agent, reflecting its limited contribution to liquid phase formation during sintering [21].

3.2 Flexural Strength

The A series, devoid of MSWI FA, exhibited the highest flexural strength among all series, as shown in Figure 3. Mix A4, incorporating the maximum GGW content of 70%, provided the highest flexural strength at both firing temperatures, reaching a maximum value of 32.85 MPa at 850°C and 36.40 MPa at 950°C. These values exceed those reported for ceramic tiles incorporating glass waste, kaolin, and additives, which generally require firing temperatures above 900°C to achieve comparable flexural strength [13]. This high flexural strength is directly related to the increased flux content and the elevated firing temperature. Both factors promote the fused bonding of the glass phase and enhance sintering at reduced temperatures while maintaining sufficiently high strength within the ceramic matrix [19]. In contrast, increasing the MSWI FA content to 10, 20, and 30% in series B, C, and D, respectively, resulted in a gradual reduction in flexural strength. Mix D1, containing the highest MSWI FA content at 30%, showed the lowest flexural strength with values of 2.18 MPa at 850°C and 4.04 MPa at 950°C. The reduction in strength arises from incomplete

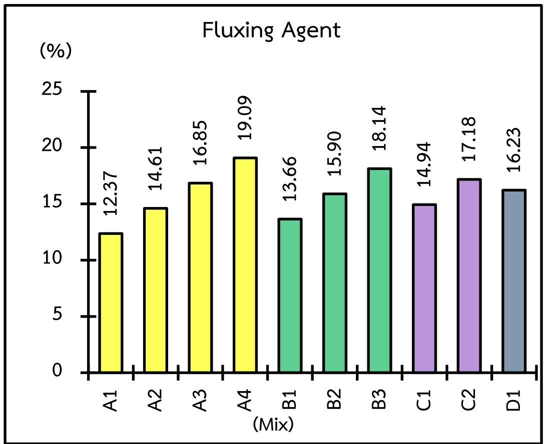

MSWI FA (%)	0	0	0	0	10	10	10	20	20	30
GGW (%)	40	50	60	70	40	50	60	40	50	40
LK (%)	60	50	40	30	50	40	30	40	30	30

Figure 2 Fluxing agent.

sintering, which hinders vitrification and generates residual porosity due to the combustion and decomposition of organic residues in MSWI FA [22]. However, MSWI FA contains hazardous heavy metals such as Hg, Pb, Zn, and Cd. Sintering above approximately 900°C has been reported to immobilize these metals within the glassy or crystalline lattice of ceramic products, thereby reducing leaching toxicity while maintaining adequate physical strength [16].

3.3 Water Absorption

As the GGW content increased from 40–70% within the A series, the water absorption consistently decreased, as depicted in Figure 4. This inverse trend is clearly evident in mixes A1 to A4 due to the strong fluxing behavior of GGW,

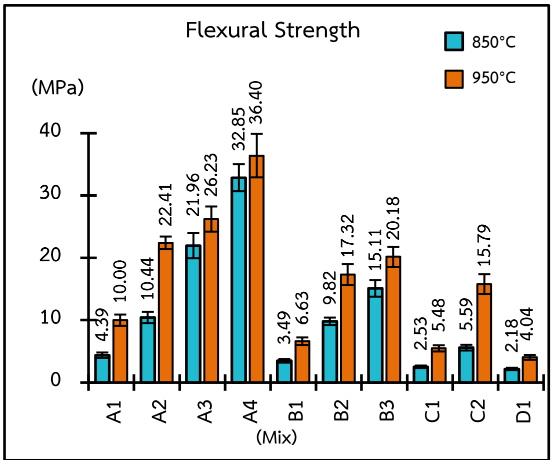

MSWI FA (%)	0	0	0	0	10	10	10	20	20	30
GGW (%)	40	50	60	70	40	50	60	40	50	40
LK (%)	60	50	40	30	50	40	30	40	30	30

Figure 3 Flexural strength.

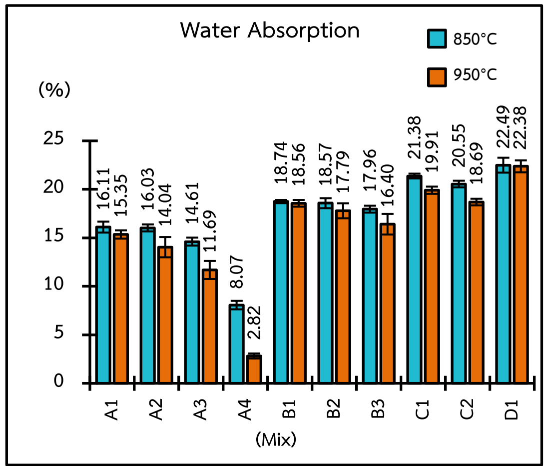

MSWI FA (%)	0	0	0	0	10	10	10	20	20	30
GGW (%)	40	50	60	70	40	50	60	40	50	40
LK (%)	60	50	40	30	50	40	30	40	30	30

Figure 4 Water absorption.

which plays the role of melting oxides and fills in the pores, thereby improving the flexural strength of specimens. This finding is consistent with previous work [23]. Conversely, the incorporation of MSWI FA, as observed by comparing the B, C, and D series with the A series, increased water absorption. This behavior results from the thermal breakdown of residual organic matter and volatile constituents in MSWI FA during firing, which generates substantial porosity within the fired bodies [24]. As a result of these combined effects, most mixes exhibited water absorption values exceeding 10%, which according to the EN 14411 standard, classifies them within group BIII. However, mix A4 was a notable exception with water absorption values of 8.07% at 850°C and 2.82% at 950°C. These values comply with the EN 14411 requirements for groups BII_b and BI_b, respectively, owing to its high GGW content, which enhances densification and reduces porosity.

3.4 Linear Shrinkage

The linear shrinkage of the specimens is significantly influenced by both the raw material compositions and the firing temperatures. At 850°C, linear shrinkage ranged from –0.37 to 5.41%, whereas firing at 950°C increased the range to –0.26 to 8.39%, as shown in Figure 5. In the A series, higher proportions of GGW correlated with substantially greater linear shrinkage due to its high content of fluxing agent, leading to extensive interparticle bonding and densification through shape shrinkage [25].

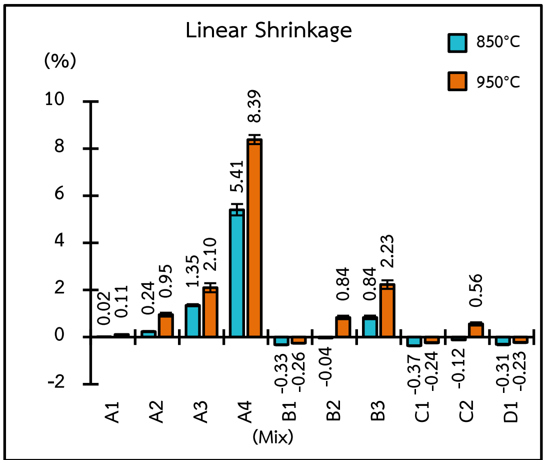

MSWI FA (%)	0	0	0	0	10	10	10	20	20	30
GGW (%)	40	50	60	70	40	50	60	40	50	40
LK (%)	60	50	40	30	50	40	30	40	30	30

Figure 5 Linear shrinkage.

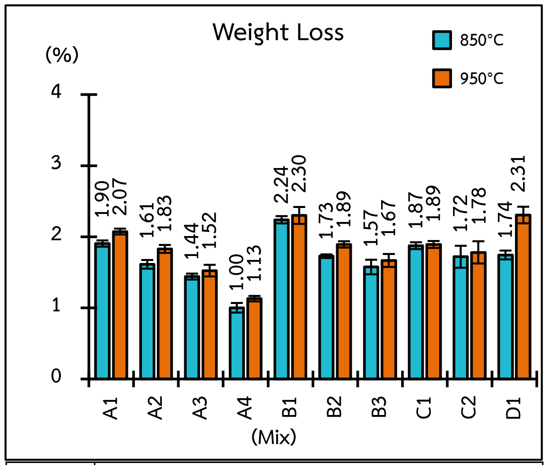

MSWI FA (%)	0	0	0	0	10	10	10	20	20	30
GGW (%)	40	50	60	70	40	50	60	40	50	40
LK (%)	60	50	40	30	50	40	30	40	30	30

Figure 6 Weight loss.

For example, mix A4 containing 70% GGW demonstrated the highest linear shrinkage of 8.39% at 950°C, as compared with 5.41% at 850°C. Meanwhile, mixtures incorporating higher amounts of MSWI FA, such as B1, B2, C1, C2, and D1, displayed slight expansion. This negative linear shrinkage, together with the markedly reduced flexural strength, indicates an overfiring effect. This phenomenon is driven by the high flux content of MSWI FA, which promotes the appearance of a substantial liquid phase accompanied by gas release during sintering. The escaping gases subsequently generate enlarged internal pores, leading to thermal expansion and slight bloating of the specimens [26].

3.5 Weight Loss

The weight loss of all mixtures showed slight variations, ranging from 1.00–2.24% and 1.13–2.31% at 850°C and 950°C, respectively, as illustrated in Figure 6. The slightly higher weight loss observed at 950°C indicates enhanced thermal decomposition at elevated temperatures. This increase is associated with the partial decomposition of alkali and/or alkaline earth metal sulfates in the raw materials. Although sulfate decomposition has been reported at approximately 1030°C [27], partial decomposition and volatile release may occur at lower temperatures. This behavior is facilitated by the presence of fluxing oxides from GGW and MSWI FA, which lower the reaction temperature. Similarly, higher proportions of MSWI FA led to a notable increase in weight loss due to the thermal degradation organic and volatile matter in MSWI FA. During firing, these substances

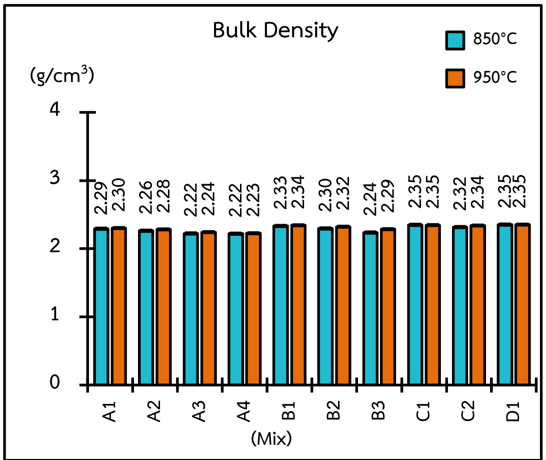

MSWI FA (%)	0	0	0	0	10	10	10	20	20	30
GGW (%)	40	50	60	70	40	50	60	40	50	40
LK (%)	60	50	40	30	50	40	30	40	30	30

Figure 7 Bulk density.

combust and release gases such as carbon dioxide (CO_2) and sulfur-containing gases (e.g., sulfur dioxide, SO_2), which contribute to additional pore generation within the ceramic matrix [28]. In contrast, weight loss decreased progressively with increasing GGW content, a trend linked to the high content of fluxing oxides and the inherent thermal stability of GGW, both of which promote extensive vitrification and the formation of a dense ceramic structure [29].

3.6 Bulk Density

The bulk density of all mixtures remained within a relatively narrow range, varying from 2.22–2.35 g/cm³ at firing temperatures of 850°C and 950°C, as illustrated in Figure 7. Increasing the firing temperature from 850–950°C resulted in a slight increase in bulk density of approximately 0.00–0.05 g/cm³, reflecting the development of a more densified sintered matrix with reduced porosity, thereby contributing to improved flexural strength. Moreover, bulk density increased with higher MSWI FA and LK contents, attributable to their relatively high specific gravity arising from the heavier mineral constituents of both materials, consistent with previous studies [29], [30]. Conversely, bulk density decreased with increasing GGW content due to the lower gravity specific of GGW compared with that of MSWI FA and LK [31].

3.7 Comparison of Flexural Strength and Water Absorption of Ceramic Tiles with the EN 14411 Standard

The flexural strength (R) and water absorption (E_v) of specimens fired at 850°C and 950°C were compared and classified in accordance with the EN 14411 standard, as summarized in Table 5.

At 850°C, mixes A3 and A4, consisting of 60% and 70% GGW without MSWI FA, satisfied the R requirements for groups BII_b and BI_b, respectively, while simultaneously meeting the E_v limits for groups BIII and BII_b. Among the mixtures containing 10% MSWI FA, only mix B3 with 60% GGW fulfilled both the R and E_v

criteria, achieving classification as group BIII. This outcome suggests that at low firing temperatures, the allowable MSWI FA content is limited to a maximum of 10% to maintain compliance with the EN 14411 standard.

At 950°C, within the A series, mixes A2, A3, and A4, containing 50–70% GGW attained the R values that met the requirements for groups BII_a, BII_a, and BI_a, respectively, while also satisfying the corresponding E_v limits for groups BIII, BIII, and BI_b. Notably, mixes B2, B3, and C2, containing 10– 20% MSWI FA complied with both the R and E_v criteria, resulting in classifications within groups BIII or BII_b. These findings demonstrate that improved physical properties at higher firing temperatures enable the incorporation of up to 20% MSWI FA while still achieving conformity with the EN 14411 standard.

3.8 Optical Microscopy (OM)

Microstructural analysis was conducted using optical microscopy to examine the surface morphology of the specimens. Observations were performed at magnifications of 150× and 300×, corresponding to scale bars of 400 µm and 200 µm, respectively. The mixes exhibiting the highest flexural strength and the lowest water absorption within each MSWI FA series, namely A4, B3, C2, and D1, were selected for OM analysis at firing temperatures of 850°C and 950°C, as presented in Figure 8 (a)–(h) and Figure 9 (a)–(h), respectively.

Table 5 Comparison of flexural strength and water absorption with the EN 14411 standard.

Mix	Firing temperature (°C)	Mixture compositions			Compliance with the EN 14411 standard			
		MSWI FA (%)	GGW (%)	LK (%)	Flexural strength (R)		Water absorption (E_v)	
					R (MPa)	Group	E_v (%)	Group
A3	850	0	60	40	21.96	BII_b	14.61	BIII
A4	850	0	70	30	32.85	BI_b	8.07	BII_b
B3	850	10	60	30	15.11	BIII	17.96	BIII
A2	950	0	50	50	22.41	BII_a	14.04	BIII
A3	950	0	60	40	26.23	BII_a	11.69	BIII
A4	950	0	70	30	36.40	BI_a	2.82	BI_b
B2	950	10	50	40	17.32	BIII	17.79	BIII
B3	950	10	60	30	20.18	BII_b	16.40	BIII
C2	950	20	50	30	15.79	BIII	18.69	BIII

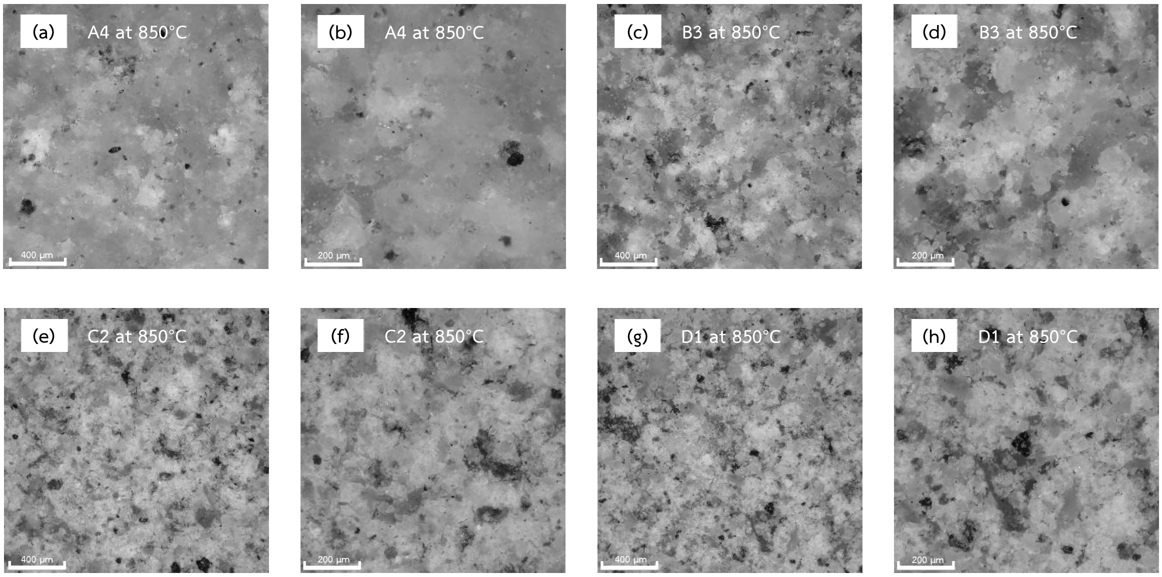

Figure 8 OM images of ceramic tiles fired at 850°C: (a, b) A4; (c, d) B3; (e, f) C2; (g, h) D1. Images (a, c, e, g) were taken at 150× (scale bar = 400 μm) and (b, d, f, h) at 300× (scale bar = 200 μm).

At 850°C, mix A4, containing 70% GGW and a high content of fluxing oxides inherent to GGW, showed a well-developed glassy phase with fused particle bonding and a dense microstructure, resulting in the highest flexural strength and the lowest water absorption among the fired specimens [12]. Mix B3, which incorporated 10% MSWI FA, displayed a reduced extent of glassy phase formation and a less compact microstructure compared with mix A4, due to its higher MSWI FA and lower GGW contents. Meanwhile, mixes C2 and D1, containing 20% and 30% MSWI FA, respectively, showed an even more pronounced presence of irregularly distributed small and large pores relative to mix B3. This increased porosity led to reduced flexural strength and increased water absorption. The formation of these additional pores is primarily attributed to the removal of organic matter and the decomposition of certain compounds in MSWI FA during firing [32].

Upon increasing the firing temperature to 950°C, all mixes exhibited greater structural densification compared with those fired at 850°C. The higher peak temperature promoted a more continuous and interconnected ceramic matrix through increased viscous flow, thereby reducing the size of interparticle pores as voids became partially filled with melt or collapsed [33].

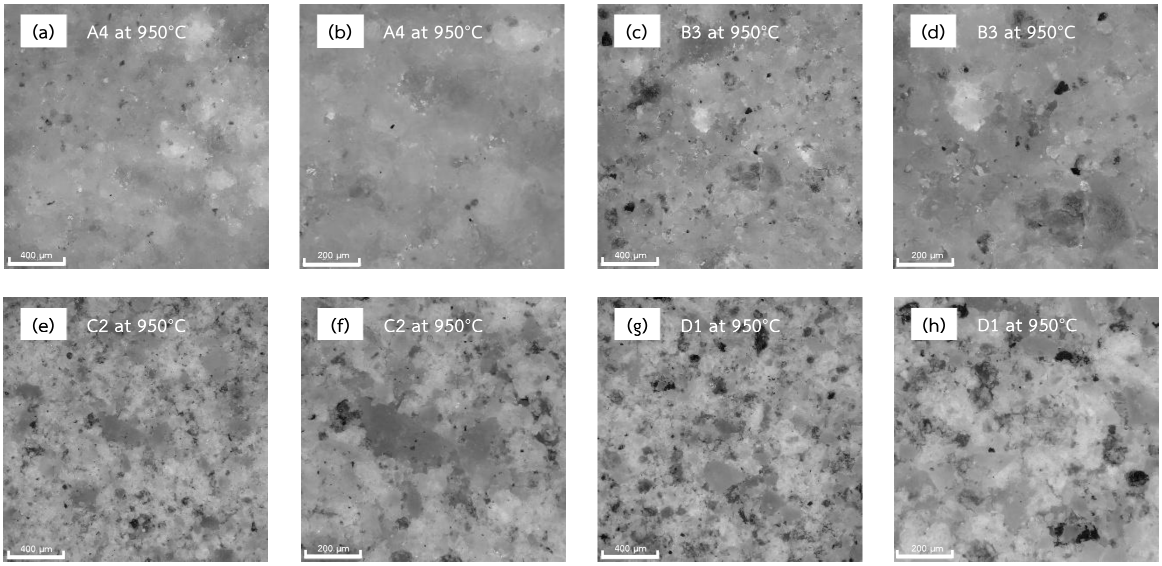

Figure 9 OM images of ceramic tiles fired at 950°C: (a, b) A4; (c, d) B3; (e, f) C2; (g, h) D1. Images (a, c, e, g) were taken at 150× (scale bar = 400 μm) and (b, d, f, h) at 300× (scale bar = 200 μm).

4. Conclusion

This study demonstrates the feasibility of producing sustainable ceramic tiles at low firing temperatures of 850°C and 950°C using a ternary mixture of MSWI FA, GGW, and LK. In the absence of MSWI FA,mixtures containing 60–70% GGW with firing at 850°C and 50–70% GGW with firing at 950°C achieved the requirements of the EN 14411 standard for both flexural strength and water absorption. In addition, mixtures incorporating up to 10% MSWI FA fired at 850°C and up to 20% MSWI FA fired at 950°C also met the relevant EN 14411 standard. Optical microscopy corroborated these results by revealing more pronounced glassy phase formation and improved densification at the higher firing temperature. The relatively high combined CaO content from GGW and MSWI FA may contribute to the immobilization of hazardous heavy metals within the ceramic matrix, potentially reducing heavy-metal leaching after sintering.

Overall, the findings highlight an effective approach for dual waste utilization as fluxing agents in low-temperature ceramic tile production, in which the combined use of GGW and MSWI FA enhances waste valorization while promoting energy-efficient manufacturing and circular resource utilization. Future research should focus on comprehensive heavy-metal leaching assessments, long-term durability and chemical stability of the tiles, advanced microstructural characterization (e.g., SEM and XRD), and optimization of compositions for large-scale industrial applications.

5. Acknowledgement

Special thanks are extended to Pattamaporn Yaikam and Pimlapat Worawong for their support regarding experimental tests. The authors are also grateful for all necessary resources by the Production and Robotics Engineering Department, Faculty of Engineering, King Mongkut's University of Technology North Bangkok, Thailand.

References

[1] S. Wang, Q. Huang, Y. Feng, and L. Wu, "Insights into the influence of waste ceramic tiles powder on cement hydration and microstructure from electrochemical impedance spectroscopy," *Frontiers in Materials*, vol. 12, 2025, Art. no. 1747505, doi: 10.3389/fmats.2025.1747505.

[2] A. Kaur, R. Bharti, and R. Sharma, "Municipal solid waste as a source of energy," in *Materials Today: Proceedings*, 2023, pp. 904–915, doi: 10.1016/j.matpr. 2021 .04.286.

[3] C. Li, P. Zhang, L. Zeng, L. Yu, and D. Li, "Study on preparation of glass-ceramics from Municipal Solid Waste Incineration (MSWI) fly ash and chromium slag," *Journal of Building Engineering*, vol. 68, Jun. 2023, Art. no. 106080, doi: 10.1016/j.jobe.2023.106080.

[4] Z. Zhang, Z. Li, Y. Yang, B. Shen, J. Ma, and L. Liu, "Preparation and characterization of fully waste-based glass-ceramics from incineration fly ash, waste glass and coal fly ash," *Ceramics International*, vol. 48, no. 15, pp. 21638–21647, Aug. 2022, doi: 10.1016/ j.ceramint.2022.04.138.

[5] S. Z. Zhao, X. Y. Zhang, B. Liu, J.-J. Zhang, H.-L. Shen, and S.-G. Zhang, "Preparation of glass–ceramics from high-chlorine MSWI fly ash by one-step process," *Rare Metals*, vol. 40, no. 11, pp. 3316–3328, Jun. 2021, doi: 10.1007/s12598-021-01770-9.

[6] K. A. Clavier, J. M. Paris, C. C. Ferraro, and T. G. Townsend, "Opportunities and challenges associated with using municipal waste incineration ash as a raw ingredient in cement production–a review," *Resources, Conservation and Recycling*, vol. 160, Sep. 2020, Art. no. 104888, doi: 10.1016/ j.resconrec.2020.104888.

[7] W. Ma, W. Shi, Y. Shi, D. Chen, B. Liu, C. Chu, D. Li, Y. Li, and G. Chen, "Plasma vitrification and heavy metals solidification of MSW and sewage sludge

incineration fly ash," *Journal of Hazardous Materials*, vol. 408, Apr. 2021, Art. no. 124809, doi: 10.1016/j.jhazmat.2020.124809.

[8] Y. Yue, J. Zhang, F. Sun, S. Wu, Y. Pan, J. Zhou, and G. Qian, "Heavy metal leaching and distribution in glass products from the co-melting treatment of electroplating sludge and MSWI fly ash," *Journal of Environmental Management*, vol. 232, pp. 226–235, Feb. 2019, doi: 10.1016/j.jenvman.2018.11.053.

[9] R. M. Khattab, M. A. Marzouk, and H. E. H. Sadek, "Synthesis and characterization of kaolin glass cullet ceramics modified with transition metal oxides for enhanced mechanical and optical properties," *Scientific Reports*, vol. 15, no. 1, pp. 19337, 2025, doi: 10.1038/s41598-025-03908-6.

[10] A. S. Ogunro, F. I. Apeh, O. C. Nwannenna, and O. Ibhadode, "Recycling of waste glass as aggregate for clay used in ceramic tile production," *American Journal of Engineering Research*, vol. 7, no. 8, pp. 272–278, 2018.

[11] Y. Liu, J. Xie, P. Hao, Y. Shi, Y. Xu, and X. Ding, "Study on factors affecting properties of foam glass made from waste glass," *Journal of Renewable Materials*, vol. 9, no. 2, pp. 237–252, 2021, doi: 10.32604/jrm.2021.012228.

[12] N. Piyarat, U. Wangrakdiskul, and P. Maingam, "Determination of the firing temperature and optimum ratio of valorizing rice husk ash, clear glass cullet and Ranong clay for developing ecological wall tiles," *Current Applied Science and Technology*, vol. 22, no. 4, pp. 1–9, Jul. 2022, doi: 10.55003/cast.2022.04.22.005.

[13] P. Maingam, U. Wangrakdiskul, and N. Piyarat, "Potential of alternative waste materials: rice husk ash and waste glass cullet with boric acid addition for low-fired unglazed tiles," *AIMS Materials Science*, vol. 8, no. 2, pp. 283–300, 2021, doi: 10.3934/matersci.2021019.

[14] X. Guo, J. Hu, and C. Wang, "Ultrasonic-assisted hydrothermal synthesis autoclaved bricks from municipal solid waste incineration fly ash and coal fly ash (MSWI-FA)," *Journal of Wuhan University of Technology–Materials Science Edition,* vol. 40, pp. 439–448, 2025, doi: 10.1007/s11595-025-3080-1.

[15] P. Sirilar, N. Srisukhumbowornchai, P. Thanakijkasem, S. Sirisoonthorn, and G. Klein, "Influence of Lampang pottery stone: Local materials in Thailand on CQF ratio, key properties, mullite formation and glaze-body fit of vitreous ceramic sanitary ware," *Journal of the Australian Ceramic*

Society, vol. 55, no. 4, pp. 1153–1160, 2019, doi: 10.1007/s41779-019-00331-9.

[16] H. Zhang, Y. Zhao, and J. Qu, "Study on use of MSWI fly ash in ceramic tile," *Journal of Hazardous Materials*, vol. 141, no. 1, pp. 106–114, Mar. 2007, doi: 10.1016/j.jhazmat.2006.06.100.

[17] *Ceramic tiles — Definition, Classification, Characteristics, Assessment and Verification of Constancy of Performance and Marking,* EN 14411:2016, 2016.

[18] J. Xu, Q. Luo, Y. Tang, Z. Zeng, and J. Liao, "Experimental study and application of controlled low-strength materials in trench backfilling in Suqian City, China," *Materials*, vol. 17, no. 4, Feb. 2024, Art. no. 775, doi: 10.3390/ma17040775.

[19] P. Chindaprasirt, A. Srisuwan, C. Saengthong, S. Lawanwadeekul, and N. Phonphuak, "Synergistic effect of fly ash and glass cullet additive on properties of fire clay bricks," *Journal of Building Engineering*, vol. 44, Dec. 2021, Art. no. 102942, doi: 10.1016 /j.jobe.2021.102942.

[20] S. He, Y. Zhou, P. Yu, X. Xia, and H. Yang, "Effects and mechanism of the conditions of sintering on heavy metal leaching characteristic in municipal solid waste incineration fly ash," *Environmental Science and Pollution Research*, vol. 29, pp. 84886–84902, 2022, doi: 10.1007/s11356-022-21804-8.

[21] S. L. Jasim, S. A. Zaidan, and E. M. Hadi, "Study the effect nano alumina on refractory manufactured from SiC and Kaolin," in *AIP Conference Proceedings*, vol. 3190, no. 1, 2025, pp. 100002, doi: 10.1063/5.0294222.

[22] V. Voišnienė, O. Kizinievič, and V. Kizinievič, "Effect of municipal solid waste incineration fly ash on the properties, microstructure and durability of clay bricks," *Ceramics-Silikáty*, vol. 64, no. 4, pp. 423–433, 2020, doi: 10.13168/cs.2020.0030.

[23] N. Piyarat, U. Wangrakdiskul, and P. Maingam, "Influence of boric acid additive on physical properties of utilizing wastes for producing eco-friendly fired clay tiles," *Key Engineering Materials*, vol. 889, 2021, pp. 183–188, doi: 10.4028/www.scientific.net/KEM.889.183.

[24] V. Voisniene, O. Kizinievic, and V. Kizinievic, "Feasibility study of using clay bricks made from municipal solid waste incinerator (Mswi) fly ash," in *IOP Conference Series: Materials Science and Engineering*, vol. 603, no. 2, 2019,

Art. no. 022058, doi: 10.1088/1757-899X/603/2/022058.

[25] J. Huang, Y. Jin, X. Chu, Z. Shu, X. Ma, and J. Liu, "Development of a loose powder sintering method for the preparation of porous ceramic from municipal solid waste incineration fly ash," *Waste Management*, vol. 169, pp. 243–252, Sep. 2023, doi: 10.1016/j.wasman.2023.06.010.

[26] W. Wons, K. Rzepa, M. Reben, and P. Murzyn, "Thermal studies of fly ashes expansion," *Journal of Thermal Analysis and Calorimetry*, vol. 143, no. 4, pp. 2883–2891, 2021, doi: 10.1007/s10973-020-09566-2.

[27] A. Polettini, R. Pomi, L. Trinci, A. Muntoni, and S. L. Mastro, "Engineering and environmental properties of thermally treated mixtures containing MSWI fly ash and low-cost additives," *Chemosphere*, vol. 56, no. 10, pp. 901–910, Sep. 2004, doi: 10.1016/j.chemosphere.2004.05.004.

[28] G. M. Kirkelund, L. Skevi, and L. M. Ottosen, "Electrodialytically treated MSWI fly ash use in clay bricks," *Construction and Building Materials*, vol. 254, no. 11, Sep. 2020, Art. no. 119286, doi: 10.1016/j.conbuildmat.2020.119286.

[29] U. Wangrakdiskul, P. Maingam, and N. Piyarat, "Eco-friendly fired clay tiles with greenish and greyish colored incorporating alternative recycled waste materials," *Key Engineering Materials*, vol. 856, 2020, pp. 376–383, doi: 10.4028/www.scientific.net/KEM.856.376.

[30] B. H. Cho, B. H. Nam, J. An, and H. Youn, "Municipal Solid Waste Incineration (MSWI) ashes as construction materials– A review," *Materials*, vol. 13, no. 14, 2020, Art. no. 3143, doi: 10.3390/ma13143143.

[31] D. E. Ewa, J. O. Ukpata, G. A. Akeke, A. A. Etika, and E. I. Adah, "Use of waste glass fines to improve rigidity ratio of asphalt," *Cogent Engineering*, vol. 9, no. 1, 2022, Art. no. 2107197, doi: 10.1080/23311916.2022.2107197.

[32] S. Zhong, L. Shen, W. Xu, Y. Fang, and Y. Pan, "Water–soaking pretreatment for enhanced performance and heavy metal immobilization in alkali– activated pyrolysis MSWIFA materials," *Materials*, vol. 18, no. 19, 2025, Art. no. 4520, doi: 10.3390/ma 18194520.

[33] K.-L. Lin and J.-C. Chang, "Feasibility of recycling waste diatomite and fly ash cosintered as porous ceramics," *Environmental Progress & Sustainable Energy*, vol. 32, no. 1, pp. 25–34, 2013, doi: 10.1002/ep.10592.